Fission of solitons in continuous-wave supercontinuum

E. J. R. Kelleher,[1,*] M. Erkintalo,[2] and J. C. Travers[3]

[1]*Femtosecond Optics Group, Department of Physics, Blackett Laboratory, Prince Consort Road, Imperial College London, London SW7 2AZ, UK*

[2]*Department of Physics, University of Auckland, Private Bag 92019, Auckland 1142, New Zealand*

[3]*Max Planck Institute for the Science of Light, Günther-Scharowsky-Str. 1/Bau 24, Erlangen D-91058, Germany*

**Corresponding author: edmund.kelleher08@imperial.ac.uk*

Received September 26, 2012; revised November 21, 2012; accepted November 21, 2012; posted November 26, 2012 (Doc. ID 176965); published December 13, 2012

We use numerical simulations to revisit the generation of fiber supercontinua pumped by partially coherent continuous-wave (CW) sources. Specifically, we show that intensity fluctuations characteristic of temporal partial coherence can be described as a stochastic train of high-order solitons, whose individual dynamics drive continuum formation. For sources with sufficiently low coherence, these solitons actually undergo fission rather than modulation instability, changing the nature of the CW supercontinuum evolution. © 2012 Optical Society of America

OCIS codes: 320.6629, 060.4370, 190.5530, 060.7140.

The generation of broadband fiber supercontinua (SC) has been widely studied, and the mechanisms leading to the rapid and extreme spectral expansion of a narrowband pump signal are generally well understood. Modulation instability (MI), the breakup of a quasi-continuous field into many fundamental solitons with small random variations in duration and intensity, has been shown to play the dominant role in the development of continua under both long-pulse and coherent and weakly incoherent continuous-wave (CW) excitation [1,2]. In contrast, for femtosecond pump pulses strong soliton-effect temporal compression, followed by fission into fundamental solitons and resonant dispersive radiation, is often the dominant mechanism.

The precise conditions that determine the dominant SC formation dynamics have been widely explored, and it is now generally accepted that the key quantity ruling the competition of fission against MI is the soliton order N: for $N < 15$, deterministic soliton fission tends to occur, while for $N \gg 15$, noise-driven MI dominates [2–6]. Because of its linear dependence on pulse duration, the soliton order of continuous waves is infinite, and therefore the initial stages of CW-pumped SC are generally understood to be fully governed by MI. However, this argument is only exact in the limit of a completely coherent, purely monochromatic single-frequency field, and it is known that even a quasi-CW field can be "forced" to exhibit fissionlike dynamics through the application of an external intensity modulation [7]. Realistic CW fiber lasers, which are commonly used for SC generation [1,8,9], do not exhibit complete temporal coherence, and although weak incoherence has been found to enhance the MI process [1,10–12], an unanswered question arises: what is the governing mechanism if the CW pump is only partially coherent, such that although it averages to a CW, it actually consists of many incoherent intensity fluctuations with a finite duration?

In this Letter, we use numerical simulations based on the generalized nonlinear Schrödinger equation to reassess the dynamical formation of CW-pumped SC. We use a realistic CW fiber laser model and highlight how the strong intensity fluctuations characteristic of partial temporal coherence can be viewed as an incoherent train of solitons, whose effective soliton orders are governed by the pump bandwidth. We find that when the effective soliton orders of the fluctuations meet the condition $2 < N_{\text{eff}} < 15$, the overall spectral expansion can be interpreted as the sum of several localized soliton-fission events, despite the CW nature of the pump.

Figure 1(a) shows the simulated evolution of an initially single-frequency CW field with power $P_0 = 6.3$ W over 50 m of propagation in a highly nonlinear fiber (HNLF), with a group-velocity dispersion of $\beta_2 = -3.3$ ps^2 km^{-1} and a nonlinear coefficient $\gamma = 12.3$ W^{-1} km^{-1} at the pump wavelength $\lambda_p = 1565$ nm. Characteristic MI sidebands are amplified from the shot-noise limited background, included in our propagation model using the conventional approach of adding a single photon with a random phase to each spectral discretization bin [2]. However, typical CW fiber lasers are not shot-noise limited or single-frequency, but exhibit strong, stochastic fluctuations in their temporal intensity that result from interactions between the many longitudinal modes within their

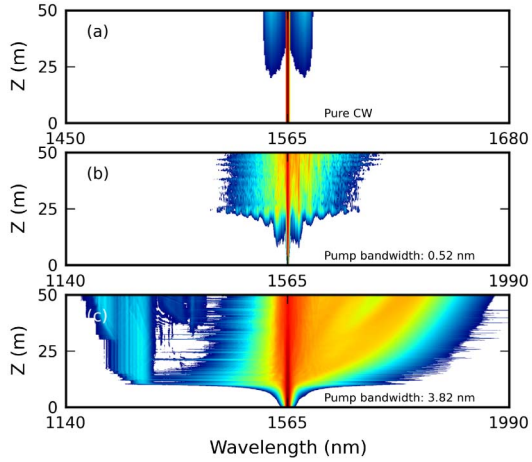

Fig. 1. (Color online) Spectral evolution of a CW field propagating in an HNLF. (a) Pure CW input signal, with one photon per mode noise. (b) Model of a realistic CW fiber laser, with a bandwidth of 0.52 nm and one photon per mode noise. (c) As per (b) but with a bandwidth of 3.82 nm. Color bar: −75 dB 0 dB.

bandwidth. A number of models exist to describe the nonlinear coupling that occurs in the cavity of a CW fiber laser [9,12–15]. Here, we proceed with the simplified forward-propagating model outlined, and shown to have good empirical validity, in [9], and depict in Fig. 1(b) the spectral evolution of a CW fiber laser with a pump bandwidth of $\Delta\lambda_p = 0.52$ nm. Note that we assume the same HNLF parameters as above throughout the text. In this case, the spectral evolution can be seen to be similar to that in Fig. 1(a), and we can again identify the amplified MI sidebands. We can also see how the sidebands are generated far more efficiently and with a larger frequency detuning due to the intensity fluctuations of the partially coherent pump [1,9,16]. It should be noted that this order of pump bandwidth is typical for CW supercontinuum generation with the most commonly used rare-earth doped fiber lasers, but is narrower than most Raman fiber lasers or amplified spontaneous emission sources.

Surprisingly, upon further increase of the pump bandwidth, the dynamics are fundamentally altered. In Fig. 1(c) we show the spectral evolution with $\Delta\lambda_p = 3.82$ nm and observe that the signature sidebands of MI are fully absent; instead rapid spectral expansion can be seen to occur after ~9.5 m of propagation.

The spectral evolution in Fig. 1(c) resembles dynamics characteristic of soliton fission, with abrupt generation of high-frequency dispersive waves and Raman-redshifting fundamental solitons. In order to gain more insight, we show in Fig. 2 the computed dynamics in the time domain for the $\Delta\lambda_p = 3.82$ nm case. We first plot in Fig. 2(a) the initial pump field, and can see how the field corresponds to a stochastic train of temporal fluctuations characterized by the coherence time $\tau_c = \lambda_p^2/(c\Delta\lambda_p) \sim 2.1$ ps. A closeup of the most intense noise spike is shown in Fig. 2(b), and is fitted with a sech^2 pulse shape—the functional form of a temporal soliton. This temporal fluctuation has an effective soliton order $N = (\gamma P_s T_s^2/|\beta_2|)^{1/2} \approx 11$, and can thus be expected to display qualitatively similar propagation dynamics to a corresponding high-order soliton. Indeed, in Fig. 2(c) we show the evolution of the fluctuation in the time domain, and can see how it undergoes significant temporal compression [shown explicitly in Fig. 2(d)] prior to fissioning into several fundamental Raman-redshifting solitons. This evolution is identical to high-order soliton propagation, which is known to be inherently unstable to perturbations such as third-order dispersion and Raman scattering.

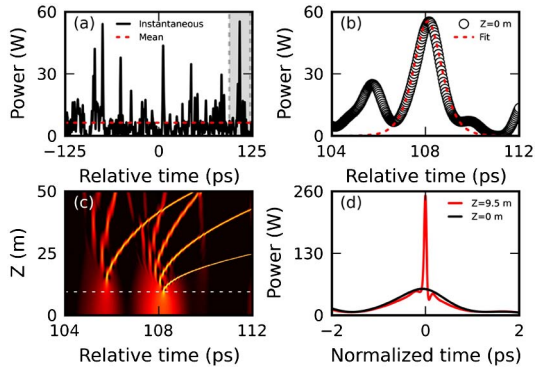

Fig. 2. (Color online) (a) Computed instantaneous and averaged power of a typical CW fiber laser, with a bandwidth of 3.82 nm. (b) Closeup on the gray shaded region in (a). The intensity is fitted with the functional shape of a temporal soliton, with a duration of $T_s = 0.8$ ps and peak power $P_s = 55.4$ W. (c) Density map showing the temporal evolution with propagation distance of the region shown in (b). Color bar: −20 dB 0 dB. (d) Temporal intensity slices at the indicated propagation distances. The white dotted line in (c) denotes the approximate point of maximal compression at 9.5 m.

Fission events as described above occur around all the localized noise pulsations that can satisfy the high-order soliton condition. As such, the noiselike input field can be viewed as an incoherent train of high-order solitons, where each spike possesses a distinct set of characteristics (soliton order, temporal duration, peak power). Correspondingly, the onset of supercontinuum generation can now be seen to arise, not from collective MI, but from a sequence of quasi-independent soliton-fission events experienced during propagation by each distinct noise fluctuation. The solitons that emerge from each fission event will, however, be very closely spaced compared to mode-locked laser-pumped SC, and will experience a large number of Raman-mediated collisions, as is characteristic of all CW SC [17].

We next examine in more detail the potential for a CW pump field of a specified bandwidth to sustain fluctuations corresponding to high-order solitons by considering a purely monochromatic field with average power P_0, discretized into time intervals spanning a single coherence time. Assuming that the energy, $E_c = P_0\tau_c$, within each interval is fully contained in a sech^2-shaped pulse, with a duration coinciding with the coherence time, we derive the following estimate for the effective soliton order:

$$N_{\text{eff}} = \left[\frac{\gamma P_0 \lambda_p^4}{2c^2 \Delta\lambda_p^2 |\beta_2|}\right]^{1/2}. \quad (1)$$

To support this approach, we have extracted the duration and peak power of the most intense noise component within the realistically modeled CW pump field, and compare in Fig. 3(a) the obtained soliton orders (circles) with the analytical estimate given by Eq. (1) (blue line) for varying pump bandwidths. For completeness, we also show in Fig. 3(a) results obtained from a simpler CW model based on a sech-shaped spectral intensity and a random spectral phase (red crosses) [12].

The analytical estimate given by Eq. (1) yields an excellent fit with the values obtained from both the rigorous and the simplified CW laser models. Moreover, we observe that the effective soliton order decreases monotonically for increasing pump bandwidth. This observation allows us to explain the fundamentally different spectral evolutions of Fig. 1: for a highly coherent source the effective soliton orders of individual noise fluctuations $N_{\text{eff}} \gg 15$, resulting in MI-dominated evolution, while for low-coherence sources $N_{\text{eff}} < 15$, such that the evolution is dominated by the quasi-independent fission of distinct fluctuations.

At this point we wish to remark that although MI results in the breakup of a quasi-CW field into a train of pulses, no subsequent fission can take place. This is

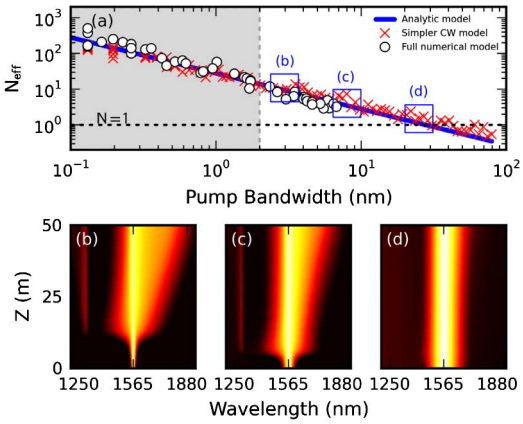

Fig. 3. (Color online) (a) Effective soliton order versus pump bandwidth. The gray region highlights bandwidths for which $N_{\text{eff}} > 15$. The blue boxes correspond to the positions of the pump fields of (b)–(d). Average spectral intensity evolution, over 100 independent realizations, as a function of propagation distance (b)–(d). Color bar: 0 dB –75 dB.

because the emanating fluctuations are bound to have soliton orders close to unity [18], which is in contrast with partially coherent pumping where the effective soliton order varies continuously with the pump bandwidth.

To further elucidate our fission-based description of CW continuum formation, we show in Figs. 3(b)–3(d) the spectral evolution for three input pump bandwidths (3 dB widths of 2.97, 8.0, and 25.0 nm), with corresponding effective soliton orders ($N_{\text{eff}} \approx 10$, 4, 1.5, respectively) represented by the three blue boxes in Fig. 3(a). The spectral evolutions shown were averaged over a stochastic ensemble size of 100. It is clear that the fission length is longest for the pump bandwidth with the largest effective soliton order [see Fig. 3(b)], but the output bandwidth is greater. This is in exact agreement with the trend reported for increasing soliton order in the context of soliton-fission driven SC generation. It is interesting to note that for a pump bandwidth $\Delta\lambda_p = 25$ nm no apparent spectral broadening takes place during the full evolution [see Fig. 3(d)]. In fact, this can be readily explained by the proximity of the effective soliton order to unity, such that in this case the individual noise fluctuations approximately correspond to fundamental, propagation-invariant solitons and can experience neither MI nor fission. Taking $N_{\text{eff}} < 2$, where neither soliton fission nor MI can occur, we can estimate that when $\Delta\lambda_p >$ 14 nm, negligible spectral broadening should occur. We note that this regime is associated with pump bandwidths exceeding the coherent MI gain bandwidth. Indeed, it can be shown that for bandwidths $2\pi\Delta\upsilon_p > [4\gamma P_0/|\beta_2|]^{1/2}$ the effective soliton order $N_{\text{eff}} < \pi/\sqrt{2}$. Of course, further increase in pump bandwidth will prohibit all soliton formation ($N_{\text{eff}} < 1$), and will result in a thermalized field as predicted by wave turbulence theory [19].

In [10] an optimal degree of pump partial coherence was found to possess a coherence time of $\tau_c = 3\tau_{\text{MI}}$, with $\tau_{\text{MI}} = (2\pi^2|\beta_2|/\gamma P_0)^{1/2}$ the MI period. Although the analysis therein was based on the relationship between the MI period and the coherence time, the optimal coherence time was determined independently using comprehensive direct numerical simulations. Using Eq. (1) we find that the corresponding effective soliton order is $N_{\text{eff}} \sim 3\pi$. Therefore, the optimum CW supercontinuum mechanism is actually within the $N \sim 10$ soliton-fission domain.

To conclude, we have shown that, in contrast to the broadly accepted description, soliton-fission-based evolution can play a role in the rich dynamics of CW supercontinuum generation. Specifically, we have shown that a partially coherent CW field can be described as an incoherent train of high-order solitons, and have suggested an equation relating the pump bandwidth to the average effective soliton order of the fluctuating field based on its coherence time. These incoherently related solitons either undergo MI or quasi-independent fission events, depending on their effective soliton order. Based on previous comprehensive numerical simulations, we have shown that the optimal degree of pump partial coherence corresponds to strong fission-based evolution.

EJRK acknowledges the UK Engineering and Physical Sciences Research Council (EPSRC) for funding support.

References

1. J. C. Travers, in *Supercontinuum Generation in Optical Fibers*, J. M. Dudley and J. R. Taylor, eds. (Cambridge University, 2010), p. 142.
2. J. M. Dudley and S. Coen, Opt. Lett. **27**, 1180 (2002).
3. J. M. Dudley, G. Genty, and S. Coen, Rev. Mod. Phys. **78**, 1135 (2006).
4. J. C. Travers, J. Opt. **12**, 113001 (2010).
5. A. Demircan and U. Bandelow, Appl. Phys. B **86**, 31 (2007).
6. G. Genty, M. Surakka, J. Turunen, and A. T. Friberg, J. Opt. Soc. Am. B **28**, 2301 (2011).
7. G. Genty and J. M. Dudley, IEEE J. Quantum Electron. **45**, 1331 (2009).
8. A. Mussot, E. Lantz, H. Maillotte, T. Sylvestre, C. Finot, and S. Pitois, Opt. Express **12**, 2838 (2004).
9. A. Mussot, A. Kudlinski, M. Kolobov, E. Louvergneaux, M. Douay, and M. Taki, Opt. Express **17**, 17010 (2009).
10. E. J. R. Kelleher, J. C. Travers, S. V. Popov, and J. R. Taylor, J. Opt. Soc. Am. B **29**, 502 (2012).
11. S. Martin-Lopez, A. Carrasco-Sanz, P. Corredera, L. Abrardi, M. L. Hernanz, and M. Gonzalez-Herraez, Opt. Lett. **31**, 3477 (2006).
12. F. Vanholsbeeck, S. Martin-Lopez, M. Gonzlez-Herrez, and S. Coen, Opt. Express **13**, 6615 (2005).
13. J. C. Travers, S. V. Popov, and J. R. Taylor, in *Conference on Lasers and Electro-Optics*, Technical Digest (CD) (Optical Society of America, 2008), p. CMT3.
14. M. Frosz, Opt. Express **18**, 14778 (2010).
15. S. K. Turitsyn, A. E. Bednyakova, M. P. Fedoruk, A. I. Latkin, A. A. Fotiadi, A. S. Kurkov, and E. Sholokhov, Opt. Express **19**, 8394 (2011).
16. A. Sauter, S. Pitois, G. Millot, and A. Picozzi, Opt. Lett. **30** 2143 (2005).
17. M. Frosz, O. Bang, and A. Bjarklev, Opt. Express **14**, 9391 (2006).
18. J. M. Dudley, G. Genty, F. Dias, B. Kibler, and N. Akhmediev, Opt. Express **17**, 21497 (2009).
19. B. Barviau, B. Kibler, and A. Picozzi, Phys. Rev. A **79** 063840 (2009).